Power-Consumption Outage in Beyond Fifth Generation Mobile Communication Systems

Power-Consumption Outage in Beyond Fifth Generation Mobile Communication Systems

Jing Yang, *Student Member, IEEE,* Xiaohu Ge, *Senior Member, IEEE,* John Thompson, *Fellow, IEEE,* Hamid Gharavi, *Life Fellow, IEEE*

***Abstract*—One of the biggest problems facing future mobile systems beyond 5G (B5G) is the energy dissipation of mobile devices at high data rates. The heat generated by these devices can impact the performance as a result of a new type of outage called power-consumption outage. In this paper, we propose a general definition of the power-consumption outage and describe its three features. Based on the heat transfer model in smartphones, the power-consumption outage probability is analyzed. Specifically, we derive the joint outage probability of channel and power-consumption outages in relation to the signal-to-noise ratio (SNR), communication duration, and initial temperature of the smartphone-back-plate. The joint outage probability is then used to obtain the upper bound of the maximum receiving rate of a typical smartphone. Furthermore, we propose and analyze the impact on the capacity of the power-consumption outage. Simulation results show that the power-consumption outage probability increases with an increase of SNR and with extension of the communication duration. The upper bound of the maximum receiving rate of a smartphone decreases with an extension of communication duration. Considering the joint outage probability, simulation results show that the outage capacities, i.e., channel and power-consumption outages, decrease with an increase of SNR after reaching a given capacity threshold.**

***Index Terms*—massive MIMO, mobile communication, outage probability, capacity with outage, smartphones.**

I. Introduction

The fifth generation (5G) mobile communication system provides gigabit-per-second (Gbps) data rates to support applications such as virtual reality (VR) and augmented reality (AR) [1]. While millimeter-wave (mmWave) communications and massive multiple-input multiple-output (MIMO) technologies have been adopted to support Gbps data rates in 5G [2], [3], demands for even higher rates will continue to dominate future generations of mobile systems well beyond 5G (B5G). Moreover, the ultra-dense network is a key deployment strategy targeting seamless coverage of 5G cellular networks [4] and reduces the outage probability of mobile communication between base stations (BSs) and mobile devices, such as smartphones. However, the heat generated by the chip computation in smartphones raises the temperature of the mobile device back-plate as the data-rate increases. Considering the maximum receiving rate of smartphones [5], a new type of outage, called power-consumption outage, is rapidly emerging [6]. Power-consumption outage is related to the heat dissipation of smartphones [6], which is different from the channel outage in which the power of a received signal falls below the target minimum level at the receiver [7]. However, the general definition and features of power-consumption outage have not been thoroughly investigated in previous studies. Therefore, it is crucial to introduce a general definition of the power-consumption outage, which will require developing a probability model, especially in 5G and B5G communication systems, which support high data rates. For instance, at these rates if communication between a base station and a smartphone is sustained for a long period of time, the temperature of the smartphone-back-plate will exceed the maximum temperature, i.e., 45 °C, that has been set to avoid burning the users' skin [8], [9]. When the back-plate temperature exceeds 45 °C, a protection measure of the smartphone is triggered to reduce heat generation by decreasing the working frequency of the chips in the smartphone. Without sufficient computational resources for signal and data processing in smartphones, the performance becomes unacceptable leading to a power-consumption outage event. Bear in mind that most previous studies have mainly focused on channel outage. For instance, the outage probability for the massive MIMO uplink with a general multi-level mixed-resolution analogue to digital converter (ADC) architecture has been investigated in [10]. In this study the ADC resolution profile optimization problem is formulated considering both BS energy consumption and outage probability. Considering device-to-device (D2D) communication technology for enabling the internet-of-things, channel outage probability was studied for D2D spectrum sharing in [11]. In addition, the channel outage probability of a spectrum sharing system with a distributed cognitive underlay single carrier system has been investigated [12]. To maximize the system utility of a MIMO non-orthogonal multiple access (NOMA), power allocation and beamforming schemes have been jointly designed based on the constraints of channel outage probability [13]. For vehicular networks, a theoretical framework to analyze the performance of vehicular D2D communication systems has been established based on channel outage probability [14]. Moreover, this theoretical framework was used to analyze the capacity of vehicular D2D communication systems [14].

In addition to channel outage, computational outage of cellular networks is proposed in [15], which is a violation

Jing Yang, Xiaohu Ge (Corresponding author) are with School of Electronic Information and Communications, Huazhong University of Science and Technology, Wuhan 430074, Hubei, P. R. China, (E-mail:yang_jing@hust.edu.cn, xhge@mail.hust.edu.cn).

John Thompson is with Institute for Digital Communications, University of Edinburgh, Edinburgh, EH9 3JL, UK (Email: john.thompson@ed.ac.uk).

Hamid Gharavi is with National Institute of Standards and Technology (NIST), Gaithersburg, MD 20899-8920, USA (Email: hamid.gharavi@nist.gov).

of a timing constraint in computational tasks due to limited computational resources. Moreover, the computational outage in many studies is mainly due to limitations of the internet service provider's network. Considering the limited computational resources for a cloud-based centralized radio access network, computational outage probability and its impact on the throughput performance were analyzed in [15]. In mobile cloud computing systems, computational outage probability, caused by limited computational resources in computation offloading, was derived in [16]. Moreover, the joint probability of channel and computational outages was also been derived in [16], where computational outage is assumed to be independent of channel outage. In [17], the system outage performance of full-duplex communications in a fog computing system was analyzed. Additionally, the computational outage probability in the fog computing system was derived in [17]. In practice, limitations in computational resources exist not only in network equipment but also in mobile devices, e.g., smartphones. Moreover, power-consumption outage is related to the computational resources of the chipsets in mobile devices. Although the concept of power-consumption outage has been recently proposed, detailed studies related to power-consumption outage are surprisingly rare in literature.

A. Related Work

The power-consumption outage relates to the power consumption and heat generation of smartphones. In terms of power consumption of smartphones, the authors in [18] proposed a hardware-based method to evaluate the power consumption of each module in Android smartphones and established the energy model for these modules. A comprehensive review of research papers regarding power consumption of smartphones was presented in [19], where the authors analyzed the ratio of power consumption for different modules. The classification of existing energy-estimation schemes for smartphone applications, including an analysis of current energy estimation schemes, has been studied in [20]. The data presented in [20] indicates that the central processing unit (CPU) of smartphones consumes the most energy under normal use conditions.

Overheating has been an important issue for the development of smartphones in the last decade. A thermo-ergonomic analysis of smartphones has been presented in [21]. Their results indicate that, when receiving and processing videos, the CPU and network chip overheat, causing a localised high-temperature area on the smartphone surface. An algorithm for real-time estimation of smartphone surface temperature has been developed by the authors in [22]. Their measurement results indicate that the temperature of the area on smartphone surfaces, near the CPU, is the highest. In [23], the authors proposed a new thermal simulator to measure the thermal distribution of smartphones. Their measurement results show that the working frequency of the CPU can be affected by the safe temperature for skin. The experimental results in [24] indicates that the working frequency of the CPU is significantly reduced when the temperature exceeds a certain threshold.

Based on the measurement results of the power consumption and heat generation of smartphones, the concept of power-consumption outage was first proposed in our prior work [6]. In addition, the simulation results presented in [6] show the impact of the power-consumption outage on wireless communication systems, in terms of total transmission time and total number of power consumption outages. However, a general definition and features of the power-consumption outage, which would require developing a statistical model of the power-consumption outage, has not yet been established.

B. Main Contribution and Paper Organization

In this paper, we aim to investigate the influence of the power-consumption outage on the performance of B5G mobile communication systems. The main novel contributions are summarized as follows.

1) A general definition of the power-consumption outage is proposed, and its three main features are described for the first time. Based on the proposed definition, the power-consumption outage probability of B5G mobile communication is then derived. The theoretical analysis shows that continuously receiving data will generate more heat and thus increase the device's temperature. Moreover, simulation results indicate that power consumption outage probability increases with an increase of signal-to-noise ratio and an extension of communication duration.
2) Since the power-consumption outage is not independent of the channel outage, a joint outage probability of channel and power-consumption is obtained, which is then used to further evaluate the performance of B5G mobile communication systems at high data rates.
3) Based on the power-consumption outage probability, the capacity accounting for the power-consumption outage is derived. Simulation results indicate that, after reaching a given capacity threshold, the capacity decreases as the SNR increases.
4) Using the joint outage probability, we derive the upper bound of the maximum receiving rate of smartphones under varying communication durations. Simulation results indicate that the upper bound of the maximum receiving rate of smartphones decreases with an extension of the communication duration.

The rest of this paper is outlined as follows: Section II describes the system model, including transmission and heat transfer models. In Section III, we propose a definition of the power-consumption outage. Moreover, power-consumption outage probability and joint outage probability are derived. The performance of B5G mobile communications between BSs and smartphones is analyzed in Section IV. Simulation results are presented in Section V. Finally, conclusions are drawn in Section VI. For clarity, the most important symbols used in this paper are summarized in Table I.

II. System Model

A. Transmission Model

For a single-user MIMO system working on mmWave band, Fig. 1 illustrates communication between a massive MIMO

TABLE I
DEFINITION OF SYMBOLS

Symbol	Definition
R_{b}, R	Spectrum efficiency (unit: bit/sec/Hz) and downlink rate (unit: bit/sec) of MIMO systems
Q_{air}	Heat dissipation power of free air convection (unit: Watt)
$Q_{\mathrm{therma}}^{\mathrm{chip}}$, Q_{AM}	Heat generation power of the chip and amplifiers (unit: Watt)
P_{BB}, P_{AP}	Power of the baseband processing and application processing (unit: Watt)
T_{chip}, T_{sur}, T_{env}	Temperature of the chip, smartphone-back-plate and environment (unit: Kelvin)
m, c_{chip}	Mass (unit: g) and specific heat (unit: J/kg·K) of the chip
A, L	Area (unit: cm^2) and length (unit: mm) of the heat sink
D	Thickness (unit: mm) of smartphone-back-plates
k_1, k_2	Thermal conductivity of the heat sink and smartphone-back-plates (unit: W/m·K)
h_{air}	Heat transfer coefficient of air (unit: W/m·K)
K_{BB}	Number of logic operations per bit for algorithms in baseband processing (unit: operations/bit)
K_{AP}	Number of logic operations per bit for programs in application processing (unit: operations/bit)
F_{bit}	Number of CPU cycles per bit (unit: cycles/bit)

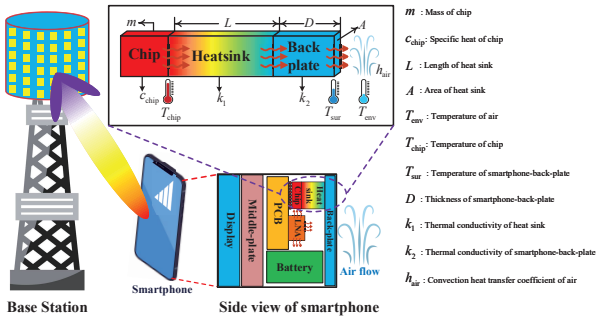

Fig. 1. Diagram of communication between a massive MIMO base station and a smartphone.

BS and a smartphone. The number of antennas in BS and the smartphone are M_{T} and M_{R}, respectively where $M_{\mathrm{T}} \gg M_{\mathrm{R}}$. The received signal at the smartphone is $\mathbf{y} \in \mathbb{C}^{M_{\mathrm{R}} \times 1}$, which is given by

$$\mathbf{y} = \mathbf{H}\mathbf{x} + \mathbf{n}, \tag{1}$$

where $\mathbf{x} \in \mathbb{C}^{M_{\mathrm{T}} \times 1}$ is the transmitted signal vector such that $\mathbb{E}\left[\mathbf{x}\mathbf{x}^{\mathrm{H}}\right] = \frac{P_{\mathrm{T}}}{M_{\mathrm{T}}}\mathbf{I}_{M_{\mathrm{T}}}$, P_{T} is the transmission power and $\mathbf{I}_{M_{\mathrm{T}}} \in \mathbb{C}^{M_{\mathrm{T}} \times M_{\mathrm{T}}}$ is the identity matrix. The matrix $\mathbf{H} \in \mathbb{C}^{M_{\mathrm{R}} \times M_{\mathrm{T}}}$ is the downlink channel complex matrix and $\mathbf{n} \in \mathbb{C}^{M_{\mathrm{R}} \times 1}$ is the random vector of additive white Gaussian noise (AWGN). The distribution of each element in $\mathbf{n}$ is a complex Gaussian distribution whose mean is zero and variance is σ^2, i.e., $\mathcal{CN}\left(0, \sigma^2\right)$. Moreover, $\mathbb{E}\left[\mathbf{n}\mathbf{n}^{\mathrm{H}}\right] = \sigma^2\mathbf{I}_{M_{\mathrm{R}}}$, where $\mathbf{I}_{M_{\mathrm{R}}} \in \mathbb{C}^{M_{\mathrm{R}} \times M_{\mathrm{R}}}$ is the identity matrix. Assuming that perfect channel state information is available at the smartphone, the downlink rate in bits/sec is given by

$$R = B\log_2 \det\left(\mathbf{I}_{M_{\mathrm{R}}} + \frac{\rho}{M_{\mathrm{T}}}\mathbf{H}\mathbf{H}^{\mathrm{H}}\right), \tag{2}$$

where B is the bandwidth and $\rho = \frac{P_{\mathrm{T}}}{\sigma^2}$ is the signal-to-noise ratio (SNR).

Considering $\mathbf{H}$ is a random matrix, the downlink rate R is a random variable. The channel outage probability is

$$\begin{aligned} p_{\mathrm{out}}(R) &= \mathbb{P}(R < R_{\mathrm{th}}) \\ &= \mathbb{P}\left[B\log_2 \det\left(\mathbf{I}_{M_{\mathrm{R}}} + \frac{\rho}{M_{\mathrm{T}}}\mathbf{H}\mathbf{H}^{\mathrm{H}}\right) < R_{\mathrm{th}}\right], \end{aligned} \tag{3}$$

where $R_{\mathrm{th}} > 0$ is the threshold rate for the downlink. The analysis of $p_{\mathrm{out}}(R)$ is based on the probability density function (PDF) of R, which has no closed-form expression for MIMO systems [25]. When the number of transmit and receive antennas increases, the spectrum efficiency of MIMO systems, R_{b}, converges to a Gaussian random variable [26]. We assume that $R_{\mathrm{b}} \sim \mathcal{N}\left(\mu, \theta^2\right)$, where $\mu = M_{\mathrm{R}}\log(1+\rho)$ and $\theta^2 = \frac{M_{\mathrm{R}}\rho^2}{M_{\mathrm{T}}(1+\rho)^2}$ [27]. Moreover, R_{b} is independent and identically distributed (*i.i.d.*) in different time slots. Considering the bandwidth B, the downlink rate is $R = BR_{\mathrm{b}}$ and the channel outage probability is calculated by

$$\begin{aligned} p_{\mathrm{out}}(R) &= \mathbb{P}(R < R_{\mathrm{th}}) = \mathbb{P}\left(R_{\mathrm{b}} < \frac{R_{\mathrm{th}}}{B}\right) \\ &= \frac{1}{2} + \frac{1}{2}\mathrm{erf}\left(\frac{\frac{R_{\mathrm{th}}}{B} - \mu}{\theta\sqrt{2}}\right) \end{aligned}, \tag{4}$$

where $\mathrm{erf}(x) = \frac{2}{\sqrt{\pi}}\int_0^x e^{-v^2}dv$ is the error function of x.

B. Heat Transfer Model

The working frequency of the CPU in smartphones decreases when the temperature of the CPU exceeds a temperature threshold [24]. Therefore, heat generated by the CPU lies at the heart of the power-consumption outage concept. Based on the measurement results in [24], the heat generated from other modules, i.e., Wi-Fi, Bluetooth and global position system (GPS), has no significant impact on the CPU temperature. Moreover, the CPU is usually integrated with a baseband processor into a core chip in existing smartphones. Considering that signal processing and application processing are executed in the baseband processor and CPU, respectively, we analyze

the heat transfer model of the core chip, and integrate the CPU with a baseband processor in the following.

In Fig. 1, the mass and specific heat of the chip in the smartphone are m (unit: g) and c_{chip} (unit: J/kg $\cdot$ K), respectively. The temperature of the chip in the smartphone is T_{chip} (unit: Kelvin). Moreover, the temperature of a smartphone-back-plate, whose area is A (unit: cm^2) and is near the chip, is T_{sur} in Fig. 1. The heat generated by the chip in the smartphone raises the temperature T_{chip}, which generates the temperature difference between T_{chip} and T_{sur}. Afterwards, the heat is transferred from the chip to the smartphone-back-plate by heat conduction. Heat conduction occurs at the heat sink, which is between the chip and the smartphone-back-plate in Fig. 1. The length, area and thermal conductivity of a heat sink are L (unit: mm), A and k_1 (unit: W/m $\cdot$ K), respectively. Moreover, the thickness and thermal conductivity of the smartphone-back-plate are; D (unit: mm) and k_2 (unit: W/m$\cdot$K), respectively. The heat, conducted to the smartphone-back-plate by the heat sink, raises the temperature T_{sur}. The rise of T_{sur} causes the temperature difference between T_{sur} and the environment temperature T_{env}, i.e., the temperature of air. Accordingly, heat accumulated in the smartphone-back-plate is dissipated by free air convection. The convection heat transfer coefficient of air is h_{air} (unit: W/m$\cdot$K). Based on a heat transfer theory [28], the heat dissipation power of free air convection for a smartphone is expressed as

$$Q_{\text{air}} = h_{\text{air}} A \left(T_{\text{sur}} - T_{\text{env}} \right), \tag{5}$$

where the unit of Q_{air} is Watt and $T_{\text{env}} \leq T_{\text{sur}} < T_{\text{safe}}$. $T_{\text{safe}} = 318$ K, i.e., 45 °C, is the maximum temperature to avoid a low-temperature burn on the users' skin [8], [9]. Additionally, T_{safe} is the upper bound of safe temperature at smartphone surface [29]. When $T_{\text{sur}} \geq T_{\text{safe}}$, protection measures in smartphones are triggered to reduce heat generation and decrease T_{sur}, e.g., decrease the working frequency of the chip [23].

In mobile communications, heat transferred by the heat sink is divided into two parts; heat generated by the chip and heat transferred from the amplifiers, i.e., low noise amplifiers (LNAs) for downlink communications and power amplifiers (PAs) for uplink communications [5]. Therefore, the total heat generation power of the chip in a smartphone is given by

$$Q_{\text{Total}} = Q_{\text{Thermal}}^{\text{chip}} + \lambda Q_{\text{AM}}, \tag{6}$$

where $Q_{\text{Thermal}}^{\text{chip}}$ (unit: Watt) is the heat generation power of the chip in a smartphone, Q_{AM} is the heat generation power of LNAs and PAs, and λ is the heat transfer ratio from LNAs and PAs to the chip. Considering that each antenna is equipped with an LNA and a PA, Q_{AM} is calculated by.

$$Q_{\text{AM}} = M_{\text{R}} \left[\zeta_{\text{DL}} P_{\text{LNA}} \left(1 - \eta_{\text{LNA}} \right) + \zeta_{\text{UL}} P_{\text{PA}} \left(1 - \eta_{\text{PA}} \right) \right], \tag{7}$$

where P_{LNA} is the power of the LNA and η_{LNA} is the efficiency of the LNA; P_{PA} is the power of the PA and η_{PA} is the efficiency of the PA; ζ_{DL} and ζ_{UL} are the fractions of downlink and uplink transmissions, respectively, with $\zeta_{\text{DL}} + \zeta_{\text{UL}} = 1$ and $0 \leq \zeta_{\text{DL}}, \zeta_{\text{UL}} \leq 1$ [30].

Based on Landauer's principle, the logically irreversible computations of chips in smartphones increases the thermodynamic entropy of the environment [31]. Considering that there is no mass flow during the computations of chips in smartphones, heat transfer is the only way to increase the thermodynamic entropy of the environment [32]. Therefore, the heat generation power of chips in smartphones $Q_{\text{Thermal}}^{\text{chip}}$ is equal to the computation power of chips P_{chip} (unit: Watt).

In Fig. 1, P_{chip} consists of three parts; the power consumed by the baseband processing, application processing and the systems' operation. The baseband processing of a smartphone mainly consists of channel decoding for the baseband processor in a downlink communication scenario. Moreover, the power consumption of channel decoding is approximately linear with the downlink rate [5]. Therefore, the power consumption of the baseband processing is calculated by

$$P_{\text{BB}} = R K_{\text{BB}} F_0 \omega E_{\text{t}}, \tag{8}$$

where K_{BB} is the number of logic operations per bit for algorithms in baseband processing, F_0 is the fan-out which is the number of loading logic gates, and ω is the activity factor of transistors for the chips in smartphones. The switch energy consumption of one transistor is E_{t} which is given by

$$E_{\text{t}} = G L_{\text{bound}}, \tag{9}$$

where $L_{\text{bound}} = k_{\text{B}} T_{\text{env}} \ln 2$ is the Landauer limit and k_{B} is the Boltzmann constant. The gap between E_{t} and L_{bound} is the constant, G, which depends on the semiconductor technology.

Considering the scenario of transmitting multimedia data, the data transmitted from a BS is decoded by the application processor in a smartphone, i.e., the CPU. Moreover, the power consumption of decoding multimedia data scales approximately linearly with the amount of multimedia data [33]. Therefore, the power consumption of the application processing is calculated by

$$P_{\text{AP}} = R K_{\text{AP}} F_0 \omega E_{\text{t}}. \tag{10}$$

$K_{\text{AP}} = N_{\text{tr}} F_{\text{bit}}$ is the number of logic operations per bit for programs in the application processing, where N_{tr} is the number of transistors in the application processor and F_{bit} is the number of central processing unit (CPU) cycles per bit [34]. Based on the results in [35], parameter F_{bit} can be modeled as a random variable with a gamma distribution for multimedia applications [36]. Therefore, the PDF of F_{bit} is given by

$$f_{\text{bit}} \left(F_{\text{bit}} \right) = \frac{1}{\beta \Gamma \left(\alpha \right)} \left(\frac{F_{\text{bit}}}{\beta} \right)^{\alpha - 1} e^{-\frac{F_{\text{bit}}}{\beta}}, \tag{11}$$

where $F_{\text{bit}} \geq 0$, α is the shape parameter and β is the scale parameter of Gamma distribution. It is assumed that F_{bit} is *i.i.d.* in different time slots.

The system operation power P_{system} is the power consumed by maintaining basic system operations and running local applications in a smartphone. Considering that no wireless link is established between the BS and each smartphone at the initial state, the smartphone maintains basic system operations and running local applications, which means that the initial value of Q_{Total} is equal to P_{system}. Assume that the initial state of the smartphone in Fig. 1 is thermal equilibrium, i.e., the

value of Q_{Total} is equal to Q_{air} at the initial state. Accordingly, the systems' operation power can be estimated by

$$P_{\text{system}} = h_{\text{air}} A \left(T_{\text{sur}}^0 - T_{\text{env}}\right), \tag{12}$$

where T_{sur}^0 is the initial temperature of T_{sur} and $T_{\text{env}} \leq T_{\text{sur}}^0 < T_{\text{safe}}$.

Therefore, the total heat generation power of chips in a smartphone is calculated by

$$\begin{aligned} Q_{\text{Total}} &= P_{\text{BB}} + P_{\text{AP}} + P_{\text{system}} + \lambda Q_{\text{AM}} \\ &= RF_0\omega E_{\text{t}} \left(K_{\text{BB}} + K_{\text{AP}}\right) + h_{\text{air}} A \left(T_{\text{sur}}^0 - T_{\text{env}}\right) + \lambda Q_{\text{AM}} \\ &= R_{\text{b}} B F_0 \omega E_{\text{t}} \left(K_{\text{BB}} + N_{\text{tr}} F_{\text{bit}}\right) + h_{\text{air}} A \left(T_{\text{sur}}^0 - T_{\text{env}}\right) + \lambda Q_{\text{AM}} \end{aligned}, \tag{13}$$

where R_{b} and F_{bit} are two independent random variables.

III. Power-Consumption Outage

In high-data-rate mobile communications, executing applications in smartphones needs a huge amount of computation, which generates significant heat in the chip. The generated heat is dissipated out of the chip by the heat sink in the smartphone. When the total heat generation power of the chip is larger than the maximum heat dissipation power of the heat sink, the temperature of chips in smartphones T_{chip} rises and exceeds the threshold temperature of chips T_{th}. In the case where $T_{\text{chip}} \geq T_{\text{th}}$, a protection measure in the smartphone is triggered to reduce heat generation by decreasing the working frequency of chips. Considering that the working frequency of the chip in smartphones is the computational resource for applications and protection measures, decreasing the working frequency would lead to computational overload, i.e., no redundant computational resources would be available to process data. The occurrence of computational overload means the smartphone performance deteriorates, e.g., poor video quality. Moreover, outage occurs when the system performance of smartphones deteriorates. Therefore, power-consumption outage is defined as the phenomenon that any reduction of working frequency triggered by the overheating of chips leads to computational overload. Under these conditions, the three features of the power-consumption outage are: overheating, decreased frequency, and overload, as described below:

1) **Overheating**: Based on Landauer's principle, the computations of chips in mobile devices increase the thermodynamic entropy of the environment by heat transfer. Overheating of chips in mobile devices indicates that a huge amount of computation has been carried out for computational tasks, e.g., signal processing, information decoding, and data processing. Furthermore, overheating raises the temperature of the chip to exceed the threshold temperature.
2) **Decreased frequency**: Generating heat is a common phenomenon in the computation of chips. To avoid the occurrence of overheating, protection measures have been built into mobile devices [37]–[39]. Decreasing the working frequency of chips is the most common protection measure [40]. For instance, when chip overheating occurs and its temperature exceeds the threshold, working frequency decreases in order to reduce the heat generation in mobile devices.
3) **Overload**: The computation capability of chips depends on its working frequency and reducing it will also decrease the chip computational resources, hence triggering the device to activate its protection measure. Under these conditions, overload occurs if there are no redundant computational resources available to execute the computational tasks. This leads to an outage in mobile devices, e.g., no redundant computational resources for signal processing, information decoding and data processing.

As smartphones are still the main mobile devices for the high-data-rate applications in 5G and B5G systems, the power-consumption outage probability of smartphones is analyzed next.

A. Power-Consumption Outage Probability

As defined earlier, power-consumption outage is measured as the likelihood of the occurrence of event $T_{\text{chip}} \geq T_{\text{th}}$. The relationship between T_{chip} and T_{sur} in Fig. 1 is derived based on heat transfer theory, which is

$$z \left(T_{\text{chip}} - T_{\text{env}}\right) = h_{\text{air}} A \left(T_{\text{sur}} - T_{\text{env}}\right), \tag{14}$$

where $z = 1/\left(\frac{L}{k_1 A} + \frac{D}{k_2 A} + \frac{1}{h_{\text{air}} A}\right)$. Based on (14) and the limit $T_{\text{sur}} < T_{\text{safe}}$, power-consumption outage does not occur based on the following condition

$$T_{\text{chip}} < \frac{h_{\text{air}} A}{z} \left(T_{\text{safe}} - T_{\text{env}}\right) + T_{\text{env}}, \tag{15}$$

which indicates: $T_{\text{th}} = \frac{h_{\text{air}} A}{z} \left(T_{\text{safe}} - T_{\text{env}}\right) + T_{\text{env}}$. Therefore, the value of T_{th} depends on T_{safe}, which means that the power-consumption outage is equal to occurrence of event; $T_{\text{sur}} \geq T_{\text{safe}}$.

Lemma 1: Suppose the initial temperature of T_{sur} is T_{sur}^0, the total heat generation power of chip in smartphones is Q_{Total}, and the communication duration is t. The temperature of T_{sur}, which varies with t in the one-dimensional non-steady-state conduction process, is given by

$$T_{\text{sur}}(t) = \frac{Q_{\text{Total}}}{h_{\text{air}} A} \left(1 - e^{-\frac{zt}{c_{\text{chip}} m}}\right) + \left(T_{\text{sur}}^0 - T_{\text{env}}\right) e^{-\frac{zt}{c_{\text{chip}} m}} + T_{\text{env}}, \tag{16}$$

where $z = 1/\left(\frac{L}{k_1 A} + \frac{D}{k_2 A} + \frac{1}{h_{\text{air}} A}\right)$.

Proof: See Appendix A.

Based on (13) and **Lemma 1**, $T_{\text{sur}}(t)$ is the function of random variables R_{b} and F_{bit}. Moreover, $T_{\text{sur}}(t)$ depends on communication duration t. Therefore, the power-consumption outage probability is the probability that $T_{\text{sur}}(t) \geq T_{\text{safe}}$ occurs, i.e., $p_{\text{out}}\left[T_{\text{sur}}(t)\right] = \mathbb{P}\left[T_{\text{sur}}(t) \geq T_{\text{safe}}\right]$.

Theorem 1: Suppose that the communication duration is t and the initial temperature of $T_{\text{sur}}(t)$ is T_{sur}^0, i.e., $T_{\text{sur}}(0) = T_{\text{sur}}^0$. The power-consumption outage probability is

$$\begin{aligned} p_{\text{out}}\left[T_{\text{sur}}(t)\right] &= \mathbb{P}\left[T_{\text{sur}}(t) \geq T_{\text{safe}}\right] \\ &= \frac{1}{2} - \frac{\int_0^{\infty} \text{erf}\left[\frac{X(F_{\text{bit}}, t) - \mu}{\theta\sqrt{2}}\right] (F_{\text{bit}})^{\alpha-1} e^{-\frac{F_{\text{bit}}}{\beta}} dF_{\text{bit}}}{2(\beta)^{\alpha} \Gamma(\alpha)}, \end{aligned} \tag{17}$$

where $X(F_{\text{bit}},t)=\frac{1}{BF_0\omega E_{\text{t}}(K_{\text{BB}}+N_{\text{tr}}F_{\text{bit}})}\left[\frac{h_{\text{air}}A\left(T_{\text{safe}}-T_{\text{sur}}^0\right)}{1-e^{-\frac{zt}{c_{\text{chip}}m}}}-\lambda Q_{\text{AM}}\right]$, $\text{erf}(x)=\frac{2}{\sqrt{\pi}}\int_0^x e^{-v^2}dv$ is the error function of x, and $\Gamma(x)=\int_0^\infty r^{x-1}e^{-r}dr$ is a gamma function of x.

Proof: Based on **Lemma 1**, the power-consumption outage probability for communication duration t is calculated by

$$\begin{aligned}&p_{\text{out}}\left[T_{\text{sur}}(t)\right]=\mathbb{P}\left[T_{\text{sur}}(t)\geq T_{\text{safe}}\right]\\&=\mathbb{P}\left[\frac{Q_{\text{Total}}}{h_{\text{air}}A}\left(1-e^{-\frac{zt}{c_{\text{chip}}m}}\right)+\left(T_{\text{sur}}^0-T_{\text{env}}\right)e^{-\frac{zt}{c_{\text{chip}}m}}+T_{\text{env}}\geq T_{\text{safe}}\right]\\&=\mathbb{P}\left[Q_{\text{Total}}\geq\frac{h_{\text{air}}A\left(T_{\text{safe}}-T_{\text{env}}\right)-h_{\text{air}}A\left(T_{\text{sur}}^0-T_{\text{env}}\right)e^{-\frac{zt}{c_{\text{chip}}m}}}{1-e^{-\frac{zt}{c_{\text{chip}}m}}}\right]\end{aligned}\tag{18}$$

Define that $Q_{\max}(t)=\frac{h_{\text{air}}A(T_{\text{safe}}-T_{\text{env}})-h_{\text{air}}A\left(T_{\text{sur}}^0-T_{\text{env}}\right)e^{-\frac{zt}{c_{\text{chip}}m}}}{1-e^{-\frac{zt}{c_{\text{chip}}m}}}$. Based on (13), the power-consumption outage probability is derived as

$$\begin{aligned}&\mathbb{P}\left[Q_{\text{Total}}\geq Q_{\max}(t)\right]\\&=\mathbb{P}\left[P_{\text{BB}}+P_{\text{AP}}+P_{\text{system}}+\lambda Q_{\text{AM}}\geq Q_{\max}(t)\right]\\&=\mathbb{E}\left\{\mathbb{P}\left[P_{\text{BB}}+P_{\text{AP}}+P_{\text{system}}+\lambda Q_{\text{AM}}\geq Q_{\max}(t)\,|F_{\text{bit}}\right]\right\}\\&=\int_0^\infty\mathbb{P}\left[P_{\text{BB}}+P_{\text{AP}}\geq Y(t)\,|F_{\text{bit}}\right]f_{\text{bit}}(F_{\text{bit}})\,dF_{\text{bit}}\\&=\int_0^\infty\mathbb{P}\left[P_{\text{BB}}+P_{\text{AP}}\geq Y(t)\,|F_{\text{bit}}\right]\frac{(F_{\text{bit}})^{\alpha-1}e^{-\frac{F_{\text{bit}}}{\beta}}}{(\beta)^\alpha\Gamma(\alpha)}dF_{\text{bit}}\end{aligned}\tag{19}$$

where $Y(t)=Q_{\max}(t)-P_{\text{system}}-\lambda Q_{\text{AM}}$. Based on (8) and (10), we can get

$$\begin{aligned}&\mathbb{P}\left[(P_{\text{BB}}+P_{\text{AP}}\geq Y(t)\,|F_{\text{bit}})\right]\\&=\mathbb{P}\left[R_{\text{b}}BF_0\omega E_{\text{t}}(K_{\text{BB}}+K_{\text{AP}})\geq Y(t)\,|F_{\text{bit}}\right]\\&=\mathbb{P}\left[R_{\text{b}}\geq\frac{Y(t)}{BF_0\omega E_{\text{t}}(K_{\text{BB}}+N_{\text{tr}}F_{\text{bit}})}|F_{\text{bit}}\right]\\&=\mathbb{P}\left[R_{\text{b}}\geq X(F_{\text{bit}},t)\,|F_{\text{bit}}\right]\end{aligned}\tag{20}$$

where $X(F_{\text{bit}},t)$ is calculated by

$$\begin{aligned}&X(F_{\text{bit}},t)=\frac{Y(t)}{BF_0\omega E_{\text{t}}(K_{\text{BB}}+N_{\text{tr}}F_{\text{bit}})}\\&=\left[\frac{h_{\text{air}}A\left(T_{\text{safe}}-T_{\text{sur}}^0\right)}{1-e^{-\frac{zt}{c_{\text{chip}}m}}}-\lambda Q_{\text{AM}}\right]\frac{1}{BF_0\omega E_{\text{t}}(K_{\text{BB}}+N_{\text{tr}}F_{\text{bit}})}\end{aligned}\tag{21}$$

Considering that R_{b} is a Gaussian random variable, i.e., $R_{\text{b}}\sim\mathcal{N}\left(\mu,\theta^2\right)$, the probability of $\mathbb{P}\left[R_{\text{b}}\geq X(F_{\text{bit}},t)\,|F_{\text{bit}}\right]$ is derived as

$$\mathbb{P}\left[R_{\text{b}}\geq X(F_{\text{bit}},t)\,|F_{\text{bit}}\right]=\frac{1}{2}-\frac{1}{2}\text{erf}\left(\frac{X(F_{\text{bit}},t)-\mu}{\theta\sqrt{2}}\right).\tag{22}$$

Based on (18), (19), (20) and (22), the equation (17) can be derived, which completes the proof.

B. Joint Outage Probability

The channel outage is a type of outage that has been well explored in mobile communication systems. The channel outage, whose probability is $\mathbb{P}(R<R_{\text{th}})$, is caused by the randomness of wireless channels where R_{th} is the threshold rate for the downlink. Under the channel outage condition (i.e., $R<R_{\text{th}}$,) the performance of mobile communication systems becomes unacceptable [7]. On the other hand, the power-consumption outage, as a new type of outage, caused by the computational overload at mobile devices, can also deteriorate the performance of mobile communication systems. As these impacts both types of outage on the performance of the communication systems, the joint outage probability of channel and power-consumption outages are investigated as follows.

Computational resources of chips in smartphones are required for computational tasks between BSs and smartphones, such as signal processing, information decoding and data processing. Without sufficient computational resources, the downlink rate; R, will be difficult to achieve. Let us define Ω as the indicator of redundant computational resources, which is a random variable. The event that there are no redundant computational resources for computational tasks is denoted as $\Omega=0$, whose probability is $\mathbb{P}(\Omega=0)$. Moreover, $\Omega=1$ is the event that indicates there are enough computational resources available to execute computational tasks where the probability is $\mathbb{P}(\Omega=1)$. Considering Ω and the channel outage, the outage probability between BSs and smartphones is calculated by

$$\begin{aligned}\mathbb{P}(\Omega R<R_{\text{th}})=&\,\mathbb{P}(\Omega R<R_{\text{th}}|\Omega=1)\,\mathbb{P}(\Omega=1)\\&+\mathbb{P}(\Omega R<R_{\text{th}}|\Omega=0)\,\mathbb{P}(\Omega=0)\end{aligned},\tag{23}$$

where $\mathbb{P}(\Omega R<R_{\text{th}}|\Omega=1)$ is the probability of event $\Omega R<R_{\text{th}}$ on condition that there are sufficient computational resources. For $\Omega=1$, the outage probability in (23) depends only on the channel outage, i.e., $\mathbb{P}(\Omega R<R_{\text{th}}|\Omega=1)=\mathbb{P}(R<R_{\text{th}}|\Omega=1)$. $\mathbb{P}(\Omega R<R_{\text{th}}|\Omega=0)$ is the probability of event, $\Omega R<R_{\text{th}}$, which is based on condition that there are no redundant computational resources available. In the case that $\Omega=0$, the computational tasks (i.e., signal processing, information decoding and data processing), cannot be executed. This consequently leads to the outage of mobile communication between BSs and smartphones, i.e., $\mathbb{P}(\Omega R<R_{\text{th}}|\Omega=0)=\mathbb{P}(0<R_{\text{th}}|\Omega=0)$ and $\mathbb{P}(0<R_{\text{th}}|\Omega=0)=1$. Therefore, (23) is converted to

$$\mathbb{P}(\Omega R<R_{\text{th}})=\mathbb{P}(R<R_{\text{th}}|\Omega=1)\,\mathbb{P}(\Omega=1)+\mathbb{P}(\Omega=0).\tag{24}$$

When the power-consumption outage occurs in smartphones, the chips has no redundant computational resources to execute the signal processing, information decoding and data processing. Therefore, the probability mass function (PMF) of Ω is assumed to be

$$\begin{cases}\mathbb{P}(\Omega=0)=\mathbb{P}\left[T_{\text{sur}}(t)\geq T_{\text{safe}}\right]\\\mathbb{P}(\Omega=1)=\mathbb{P}\left[T_{\text{sur}}(t)<T_{\text{safe}}\right]=1-\mathbb{P}\left(T_{\text{sur}}(t)\geq T_{\text{safe}}\right)\end{cases},\tag{25}$$

which indicates that the occurrence of event $\Omega=0$ is caused by event $T_{\text{sur}}\geq T_{\text{safe}}$, i.e., the power-consumption outage.

Based on (25), we derive that

$$\begin{aligned}&\mathbb{P}\left(\Omega R < R_{\text{th}}\right)\\&= \mathbb{P}\left[R < R_{\text{th}} | T_{\text{sur}}\left(t\right) < T_{\text{safe}}\right]\mathbb{P}\left[T_{\text{sur}}\left(t\right) < T_{\text{safe}}\right]\\&\quad + \mathbb{P}\left[T_{\text{sur}}\left(t\right) \geq T_{\text{safe}}\right] \qquad , \quad (26)\\&= \mathbb{P}\left[R < R_{\text{th}}, T_{\text{sur}}\left(t\right) < T_{\text{safe}}\right] + \mathbb{P}\left[T_{\text{sur}}\left(t\right) \geq T_{\text{safe}}\right]\\&= p_{\text{out}}\left[R, T_{\text{sur}}\left(t\right)\right]\end{aligned}$$

which is the joint outage probability of channel and power-consumption outages. In (26), the joint outage probability, $p_{\text{out}}\left[R, T_{\text{sur}}\left(t\right)\right]$, is the probability that any of events $T_{\text{sur}}\left(t\right) \geq T_{\text{safe}}$ and $R < R_{\text{th}}$ will occur, i.e., $\mathbb{P}\left[T_{\text{sur}}\left(t\right) \geq T_{\text{safe}} \cup R < R_{\text{th}}\right]$.

Based on **Lemma 1** and (13), the event $T_{\text{sur}}\left(t\right) < T_{\text{safe}}$ is equal to the event

$$\begin{aligned}R < &\frac{1}{F_0 \omega E_{\text{t}}\left(K_{\text{BB}} + N_{\text{tr}} F_{\text{bit}}\right)}\left[\frac{h_{\text{air}} A\left(T_{\text{safe}} - T_{\text{sur}}^0\right)}{1 - e^{-\frac{zt}{c_{\text{chip}} m}}} - \lambda Q_{\text{AM}}\right],\\&= R_{\max}\left(t\end{aligned} \tag{27}$$

which indicates that $\mathbb{P}\left[T_{\text{sur}}\left(t\right) < T_{\text{safe}}\right] = \mathbb{P}\left[R < R_{\max}\left(t\right)\right]$. Moreover, the event $T_{\text{sur}}\left(t\right) \geq T_{\text{safe}}$ is equal to the event $R \geq R_{\max}\left(t\right)$, i.e., $\mathbb{P}\left[T_{\text{sur}}\left(t\right) \geq T_{\text{safe}}\right] = \mathbb{P}\left[R \geq R_{\max}\left(t\right)\right]$. Based on (27), $R_{\max}\left(t\right)$ is a random variable, which is the function of the communication duration t and random variable F_{bit}. Defining $a = F_0 \omega E_{\text{t}} N_{\text{tr}}$, $b = F_0 \omega E_{\text{t}} K_{\text{BB}}$ and $c\left(t\right) = \frac{h_{\text{air}} A\left(T_{\text{safe}} - T_{\text{sur}}^0\right)}{1 - e^{-\frac{zt}{c_{\text{chip}} m}}} - \lambda Q_{\text{AM}}$, the expression of the random variable $R_{\max}\left(t\right)$ is converted to $R_{\max}\left(t\right) = \frac{c(t)}{a F_{\text{bit}} + b}$.

Theorem 2: Suppose that $c\left(t\right) \geq 0$. The PDF of the random variable $R_{\max}\left(t\right)$ is

$$\begin{aligned}&f\left[R_{\max}\left(t\right)\right] =\\&\frac{c\left(t\right)}{a\beta^{\alpha}\Gamma\left(\alpha\right) R_{\max}^2(t)}\left(\frac{c\left(t\right)}{a R_{\max}\left(t\right)} - \frac{b}{a}\right)^{\alpha - 1} e^{-\left(\frac{c(t)}{a\beta R_{\max}(t)} - \frac{b}{a\beta}\right)},\end{aligned} \tag{28}$$

where $0 \leq R_{\max}\left(t\right) \leq \frac{c(t)}{b}$. The cumulative distribution function (CDF) of the random variable $R_{\max}\left(t\right)$ is

$$\begin{aligned}&\mathbb{P}\left[R_{\max}\left(t\right) \leq r\right]\\&= \begin{cases}\int_{\Lambda}^{\infty} \frac{1}{\beta\Gamma(\alpha)}\left(\frac{F_{\text{bit}}}{\beta}\right)^{\alpha - 1} e^{-\frac{F_{\text{bit}}}{\beta}} dF_{\text{bit}}, & 0 \leq r \leq \frac{c(t)}{b},\\ 1, & r > \frac{c(t)}{b}\end{cases}\end{aligned} \tag{29}$$

where $\Lambda = \frac{c(t) - br}{ar}$.

Proof: See Appendix B.

Lemma 2: Suppose that $c\left(t\right) \geq 0$. Based on **Theorem 2**, the probability that both events $R < R_{\text{th}}$ and $T_{\text{sur}}\left(t\right) < T_{\text{safe}}$ occur simultaneously is (30).

Proof: See Appendix C.

When $c\left(t\right) < 0$, we get $R_{\max}\left(t\right) < 0$. Considering $R > 0$, we derive that $\mathbb{P}\left[R \geq R_{\max}\left(t\right)\right] = 1$, i.e., $\mathbb{P}\left[T_{\text{sur}}\left(t\right) \geq T_{\text{safe}}\right] = 1$ and $\mathbb{P}\left[T_{\text{sur}}\left(t\right) < T_{\text{safe}}\right] = 0$. Based on (26), $\mathbb{P}\left[R < R_{\text{th}}, T_{\text{sur}}\left(t\right) < T_{\text{safe}}\right] = 0$ and $p_{\text{out}}\left[R, T_{\text{sur}}\left(t\right)\right] = 1$ in the case of $c\left(t\right) < 0$.

Therefore, the joint outage probability of channel and power-consumption outages is calculated by (31).

The joint outage probability of channel and power-consumption outages depends on the values of R and $R_{\max}\left(t\right)$. For a special case, $R_{\max}\left(t\right) = R_{\text{th}}$, and based on (26) and (27), we derive the analytical expression of equation (30) as $\mathbb{P}\left[R < R_{\text{th}}, T_{\text{sur}}\left(t\right) < T_{\text{safe}}\right] = \mathbb{P}\left[R < R_{\text{th}}\right]$.

Subsequently, equation (31) is calculated as

$$\begin{aligned}&p_{\text{out}}\left[R, T_{\text{sur}}\left(t\right)\right]\\&= \mathbb{P}\left[R < R_{\text{th}}, T_{\text{sur}}\left(t\right) < T_{\text{safe}}\right] + \mathbb{P}\left[T_{\text{sur}}\left(t\right) \geq T_{\text{safe}}\right]\\&= \mathbb{P}\left[R < R_{\text{th}}\right] + \mathbb{P}\left[R \geq R_{\max}\left(t\right)\right] \qquad , \quad (32)\\&= \mathbb{P}\left[R < R_{\text{th}}\right] + \mathbb{P}\left[R \geq R_{\text{th}}\right]\\&= 1\end{aligned}$$

which ensures an outage occurrence in the special case: $R_{\max}\left(t\right) = R_{\text{th}}$.

IV. Performance of Mobile communications

A. The Maximum Receiving Rate of Smartphones

Based on **Lemma 1**, event $T_{\text{sur}}\left(t\right) \geq T_{\text{safe}}$ is equal to event $Q_{\text{Total}} \geq Q_{\max}\left(t\right)$ where $Q_{\max}\left(t\right)$ is

$$Q_{\max}\left(t\right) = \frac{h_{\text{air}} A\left(T_{\text{safe}} - T_{\text{env}}\right) - h_{\text{air}} A\left(T_{\text{sur}}^0 - T_{\text{env}}\right) e^{-\frac{zt}{c_{\text{chip}} m}}}{1 - e^{-\frac{zt}{c_{\text{chip}} m}}}. \tag{33}$$

$Q_{\max}\left(t\right)$ is defined as the maximum heat dissipation power of smartphones in the case where the communication duration is t. Under such condition, the power-consumption outage occurs when the value of Q_{Total} becomes larger than the value of $Q_{\max}\left(t\right)$. Therefore, $Q_{\max}\left(t\right)$ is the energy limit, under time constraint t, for the mobile communications between BSs and smartphones.

In **Theorem 2**, $R_{\max}\left(t\right)$ is defined as the maximum receiving rate of a smartphone in the case where the communication duration is t. Based on **Lemma 1** and (13), the relationship between $R_{\max}\left(t\right)$ and $Q_{\max}\left(t\right)$ is derived as

$$R_{\max}\left(t\right) = \frac{Q_{\max}\left(t\right) - P_{\text{system}} - \lambda Q_{\text{AM}}}{F_0 \omega E_{\text{t}}\left(K_{\text{BB}} + K_{\text{AP}}\right)}. \tag{34}$$

Based on **Theorem 2**, the PDF and CDF of the maximum receiving rate of a smartphone is obtained. Considering that $\mathbb{P}\left[R_{\max}\left(t\right) \leq r\right] = 1$ in the case of $r > \frac{c(t)}{b}$, the upper bound of $R_{\max}\left(t\right)$ is given by

$$\begin{aligned}R_{\max}^{\text{upper}}\left(t\right) &= \frac{c\left(t\right)}{b}\\&= \frac{1}{F_0 \omega E_{\text{t}} K_{\text{BB}}}\left[\frac{h_{\text{air}} A\left(T_{\text{safe}} - T_{\text{sur}}^0\right)}{1 - e^{-\frac{zt}{c_{\text{chip}} m}}} - \lambda Q_{\text{AM}}\right].\end{aligned} \tag{35}$$

Moreover, the outage of mobile communications occurs in the case of $R_{\max}^{\text{upper}}\left(t\right) < 0$.

The maximum receiving rate of a smartphone $R_{\max}\left(t\right)$ is the rate at which the data can be stably processed by the chipset [5], which is different from the definition of the wireless channel capacity. When the value of the communication duration is t, the outage of mobile communications occurs if $R \geq R_{\max}\left(t\right)$. Therefore, the downlink rate at the time t has to satisfy $R_{\text{th}} \leq R < R_{\max}\left(t\right)$ to avoid an outage of mobile communications.

$$\mathbb{P}\left[R < R_{\text{th}}, T_{\text{sur}}(t) < T_{\text{safe}}\right] = \begin{cases} \int_0^{R_{\text{th}}} \left[\frac{1}{2} + \frac{1}{2}\text{erf}\left(\frac{R_{\max}(t) - B\mu}{B\theta\sqrt{2}}\right)\right] f\left[R_{\max}(t)\right] dR_{\max}(t) & 0 < R_{\text{th}} \leq \frac{c(t)}{b}. \\ + p_{\text{out}}(R)\, \mathbb{P}\left[R_{\max}(t) > R_{\text{th}}\right], & \\ \mathbb{P}\left[T_{\text{sur}}(t) < T_{\text{safe}}\right], & R_{\text{th}} > \frac{c(t)}{b} \end{cases} \tag{30}$$

$$p_{\text{out}}\left[R, T_{\text{sur}}(t)\right] = \begin{cases} \int_0^{R_{\text{th}}} \left[\frac{1}{2} + \frac{1}{2}\text{erf}\left(\frac{R_{\max}(t) - B\mu}{B\theta\sqrt{2}}\right)\right] f\left[R_{\max}(t)\right] dR_{\max}(t) & 0 < R_{\text{th}} \leq \frac{c(t)}{b}. \\ + p_{\text{out}}(R)\, \mathbb{P}\left[R_{\max}(t) > R_{\text{th}}\right] + p_{\text{out}}\left[T_{\text{sur}}(t)\right], & \\ 1, & R_{\text{th}} > \frac{c(t)}{b} \end{cases} \tag{31}$$

B. Capacity with Outage

The capacity with outage is relevant to the design of mobile communication systems. Capacity with channel outage is defined as the maximum transmission rate over a channel with some channel outage probability [7]. The capacity with channel outage is given as

$$C_R^{\text{out}} = \left[1 - p_{\text{out}}(R)\right] R_{\text{th}}. \tag{36}$$

where $R_{\text{th}} = M_{\text{R}} B \log(1 + \rho_{\text{th}})$, ρ_{th} is the threshold SNR for the downlink. The outage of mobile communications depends not only on the channel state of downlink, but also on the heat dissipation of mobile devices. Considering the joint outage probability $p_{\text{out}}\left[R, T_{\text{sur}}(t)\right]$, the capacity with channel outage is rewritten as

$$C_{R,T_{\text{sur}}}^{\text{th}}(t) = \left\{1 - p_{\text{out}}\left[R, T_{\text{sur}}(t)\right]\right\} R_{\text{th}}. \tag{37}$$

Based on (26), $p_{\text{out}}\left[R, T_{\text{sur}}(t)\right] \geq p_{\text{out}}(R)$. Therefore, $C_{R,T_{\text{sur}}}^{\text{th}}(t) \leq C_R^{\text{out}}$ and $C_{R,T_{\text{sur}}}^{\text{th}}(t) = C_R^{\text{out}}$, in the case of $p_{\text{out}}\left[T_{\text{sur}}(t)\right] = 0$.

By comparison to the definition of the capacity with channel outage, the capacity with power-consumption outage is defined as the maximum receiving rate of mobile devices that the received data from BSs can be stably processed by the processor in mobile devices with incorporating power-consumption outage probability. Considering smartphones, the capacity with power-consumption outage is expressed as

$$C_{T_{\text{sur}}}^{\text{out}}(t) = \left\{1 - p_{\text{out}}\left[T_{\text{sur}}(t)\right]\right\} R_{\max}^{\text{th}}(t), \tag{38}$$

where $R_{\max}^{\text{th}}(t)$ is the threshold value of $R_{\max}(t)$, i.e., the value of $R_{\max}(t)$ in the case of $F_{\text{bit}} = F_{\text{bith,th}}$. $F_{\text{bith,th}}$ is the threshold CPU cycles for each bit. Considering the joint outage probability $p_{\text{out}}\left[R, T_{\text{sur}}(t)\right]$, the capacity with power-consumption outage is rewritten as

$$C_{R,T_{\text{sur}}}^{\max}(t) = \left\{1 - p_{\text{out}}\left[R, T_{\text{sur}}(t)\right]\right\} R_{\max}^{\text{th}}(t). \tag{39}$$

Based on (26), $p_{\text{out}}\left[R, T_{\text{sur}}(t)\right] \geq p_{\text{out}}\left[T_{\text{sur}}(t)\right]$. Therefore, $C_{R,T_{\text{sur}}}^{\max}(t) \leq C_{T_{\text{sur}}}^{\text{out}}(t)$ and $C_{R,T_{\text{sur}}}^{\max}(t) = C_{T_{\text{sur}}}^{\text{out}}(t)$, in the case of $p_{\text{out}}(R) = 0$.

V. Simulation Results

The numerical results of power-consumption outage are investigated in this section. In our simulations, we adopt the 5-nanometer semiconductor technology for the chip in the smartphones where the value of G is estimated to be 454.2 [41]. The smartphone chipset is packaged with polyethylene terephthalate (PET) whose specific heat is 1030 J/kg·K [6], i.e., $c_{\text{chip}} = 1030$ J/kg$\cdot$K. We assume the heat sink in smartphones is made of copper whose thermal conductivity is 401 W/m$\cdot$K [28], i.e., $k_1 = 401$ W/m$\cdot$K. In addition, the material used in the smartphone-back-plate is assumed to be 7075-T6 aluminum, an aluminum alloy whose thermal conductivity is 130 W/m$\cdot$K [42], i.e., $k_2 = 130$ W/m$\cdot$K. Moreover, the convection heat transfer coefficient of air is 26.3 W/m$\cdot$K [28], i.e., $h_{\text{air}} = 26.3$ W/m$\cdot$K. The default values of $\rho_{\text{th}} = 1$ dB, $F_{\text{bith,th}} = 0.1$, $\zeta_{\text{DL}} = 1$, and $T_{\text{sur}}^0 = T_{\text{env}}$ are configured in the simulations. Other default values of parameters are listed in Table II.

TABLE II
Simulation Parameters

Parameters	Values
Number of antennas in BSs M_{T}	128
Number of antennas in smartphones M_{R}	4
Bandwidth B	1 GHz
Mass of chip m	1 g
Length of heat sink L	2 mm
Area of heat sink A	1 cm^2
Thickness of smartphone-back-plate D	1 mm
Power of LNA P_{LNA}	24.3 mW
Efficiency of LNA η_{LNA}	59 %
Ratio of the heat transferred from amplifiers to the chip λ	30 %
Fanout F_0	4
Activity factor of transistors ω	0.2
Number of transistors N_{tr}	10^8
Shape parameter α	1
Scale parameter β	0.1
Environment temperature T_{env}	300 K

The channel outage probability $p_{\text{out}}(R)$ with respect to SNR and communication duration t is shown in Fig. 2. As can be seen from this figure, the value of $p_{\text{out}}(R)$ decreases as SNR increases. We can also observe that the value of $p_{\text{out}}(R)$ is independent of the communication duration.

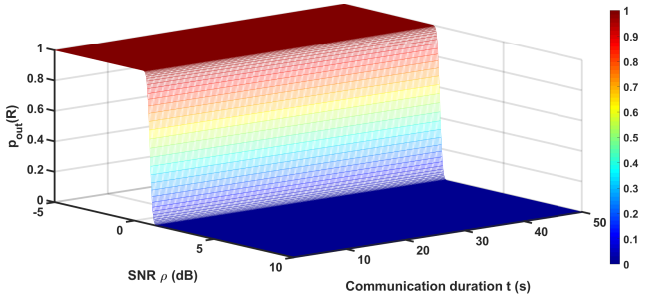

Fig. 2. Channel outage probability with respect to SNR and communication duration.

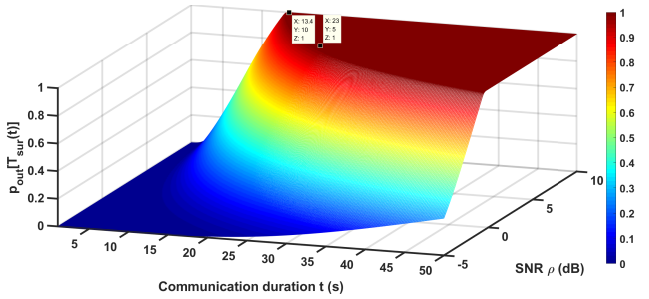

Fig. 3. Power-consumption outage probability as a function of SNR and communication duration.

Fig. 3 illustrates the power-consumption outage probability, $p_{\text{out}}\left[T_{\text{sur}}\left(t\right)\right]$, as a function of SNR and communication duration. From Figs. 2 and 3, we can observe that distributions; $p_{\text{out}}\left[T_{\text{sur}}\left(t\right)\right]$ and $p_{\text{out}}\left(R\right)$ are different. The results in Fig. 3 indicate that the value of $p_{\text{out}}\left[T_{\text{sur}}\left(t\right)\right]$ increases with an increase of SNR, when the communication duration is fixed whereas the value of $p_{\text{out}}\left[T_{\text{sur}}\left(t\right)\right]$ is dependent on the communication duration. More specifically, $p_{\text{out}}\left[T_{\text{sur}}\left(t\right)\right]$ with respect to SNR ρ has different distributions for different values of t. When the value of ρ is fixed, the value of $p_{\text{out}}\left[T_{\text{sur}}\left(t\right)\right]$ increases with an extension of the communication duration. For a fixed value of $p_{\text{out}}\left[T_{\text{sur}}\left(t\right)\right]$, the results in Fig. 3 show that the communication duration is shortened by increasing SNR. When $\rho = 5$ dB, the power-consumption outage occurs, with $p_{\text{out}}\left[T_{\text{sur}}\left(t\right)\right] = 1$, in the case of $t \geq 23$ s. When $\rho = 10$ dB, the power-consumption outage occurs, with $p_{\text{out}}\left[T_{\text{sur}}\left(t\right)\right] = 1$, for $t \geq 13.4$ s.

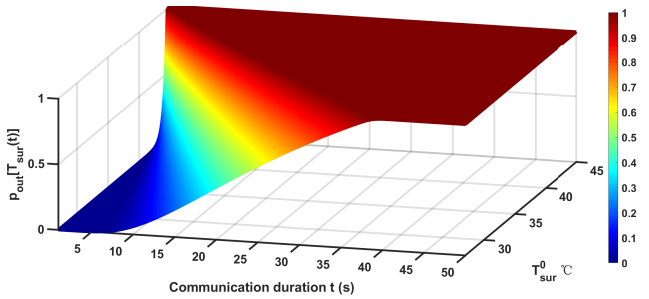

Fig. 4. Power-consumption outage probability as a function of initial temperature of smartphone-back-plate and communication duration.

The power-consumption outage probability; as a function of the initial temperature of the smartphone-back-plate T_{sur}^{0} and communication duration t is shown in Fig. 4. When the value of t is fixed, the value of $p_{\text{out}}\left[T_{\text{sur}}\left(t\right)\right]$ increases with the rise of T_{sur}^{0}, i.e., a power-consumption outage occurs easily at a high temperature of T_{sur}^{0}. Considering a fixed value of

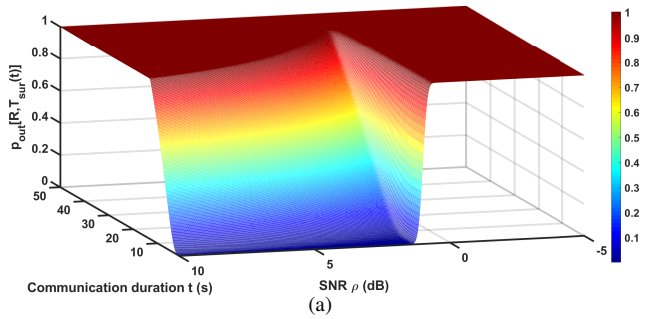

(a)

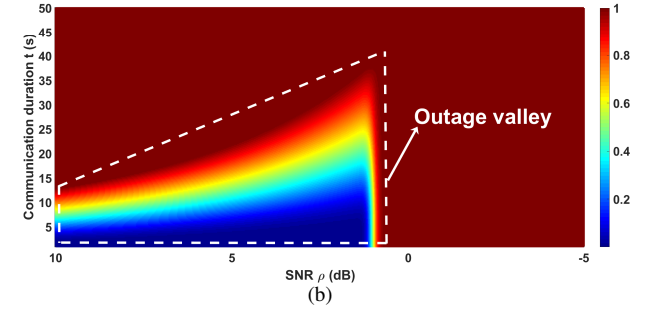

(b)

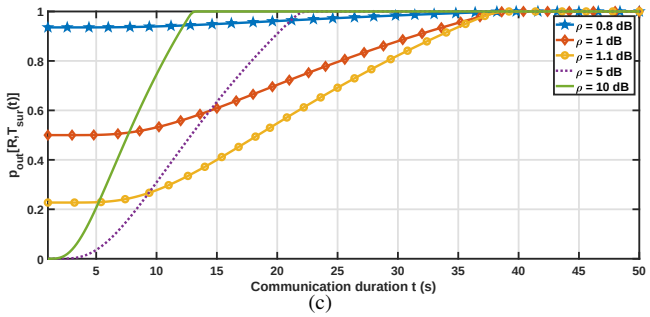

(c)

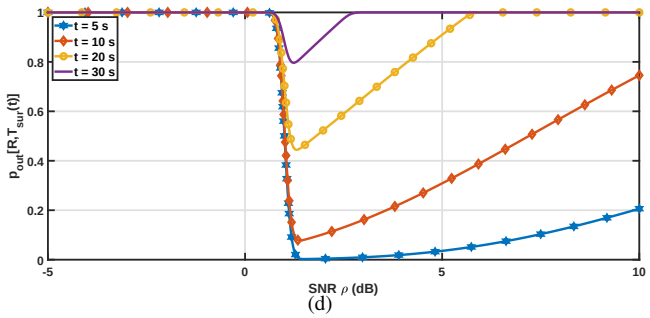

(d)

Fig. 5. (a) Joint outage probability as a function of SNR and communication duration; (b) contour plot of joint outage probability; (c) joint outage probability vs. communication duration; (d) joint outage probability vs. SNR.

$p_{\text{out}}\left[T_{\text{sur}}\left(t\right)\right]$, the results in Fig. 4 show that the communication duration is reduced as the temperature of T_{sur}^{0} increases. Based on the results in Figs. 3 and 4, the power-consumption outage probability depends on the values of ρ, T_{sur}^{0} and t.

Fig. 5 illustrates the joint outage probability; $p_{\text{out}}\left[R, T_{\text{sur}}\left(t\right)\right]$ with respect to SNR ρ and communication duration t. The contour plot of Fig. 5(a) is shown in Fig. 5(b). The results shown in Fig. 5(b) indicate that the channel and power-consumption outages create a valley in the distribution of $p_{\text{out}}\left[R, T_{\text{sur}}\left(t\right)\right]$, which we call it the outage valley. Fig. 5(c) shows $p_{\text{out}}\left[R, T_{\text{sur}}\left(t\right)\right]$ with respect to the communi-

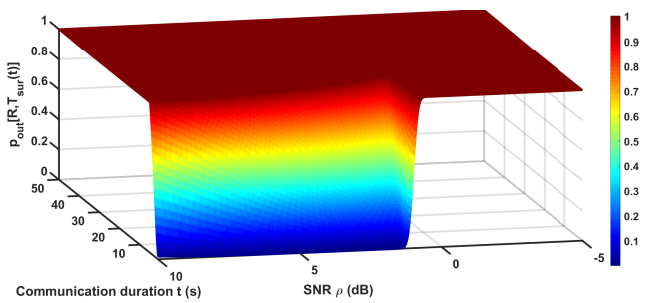

(a)

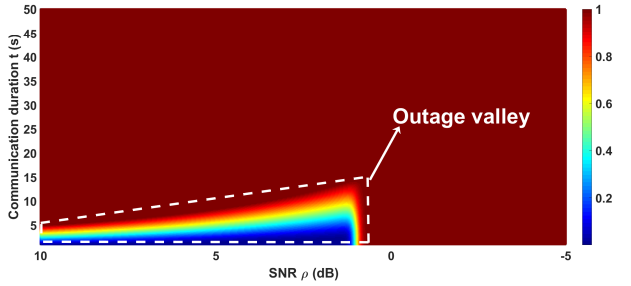

(b)

Fig. 6. (a) Joint outage probability as a function of SNR and communication duration, considering that $T_{\text{sur}}^0 = 311$ K; (b) contour plot of joint outage probability.

cation duration, t. Based on these results, the value of $p_{\text{out}}\left[R, T_{\text{sur}}\left(t\right)\right]$ increases with an extension of communication duration when $p_{\text{out}}\left[R, T_{\text{sur}}\left(t\right)\right] \neq 1$. Considering that channel outage is independent of communication duration (see in Fig. 2), the results shown in Fig. 5(c) indicate that the value of $p_{\text{out}}\left[R, T_{\text{sur}}\left(t\right)\right]$ is affected by the power-consumption outage in the time scale, i.e., the communication duration. Fig. 5(d) shows $p_{\text{out}}\left[R, T_{\text{sur}}\left(t\right)\right]$ versus SNR. In this figure, the value of $p_{\text{out}}\left[R, T_{\text{sur}}\left(t\right)\right]$ first decreases with the increase of SNR and then grows after a certain point, which is the minimum value of $p_{\text{out}}\left[R, T_{\text{sur}}\left(t\right)\right]$. Moreover, the minimum value of $p_{\text{out}}\left[R, T_{\text{sur}}\left(t\right)\right]$ increases with an extension of the communication duration.

For $T_{\text{sur}}^0 = 311$ K, i.e., 38 °C, the joint outage probability $p_{\text{out}}\left[R, T_{\text{sur}}\left(t\right)\right]$ with respect to SNR and communication duration is illustrated in Fig. 6(a). Moreover, the contour plot of Fig. 6(a) is shown in Fig. 6(b). A comparison of the results in Fig. 5(b) and Fig. 6(b) show that the area of outage valley in the contour plot shrinks with raising temperatures; T_{sur}^0. Based on the results in Fig. 5(b) and Fig. 6(b), the outage valley is a space where $p_{\text{out}}\left[R, T_{\text{sur}}\left(t\right)\right] < 1$. Moreover, the outage valley depends on the SNR ρ, the communication duration t, and the joint outage probability $p_{\text{out}}\left[R, T_{\text{sur}}\left(t\right)\right]$.

Considering the maximum receiving rate of smartphones with power-consumption outage probability, the downlink rate has to be less than the value of $R_{\max}^{\text{upper}}\left(t\right)$ whose communication duration is t. The upper bound of the maximum receiving rate of smartphones with respect to the communication duration t is illustrated in Fig. 7. The results in this figure show that the value of $R_{\max}^{\text{upper}}\left(t\right)$ decreases with an extension of the communication duration. When the value of t is fixed, the

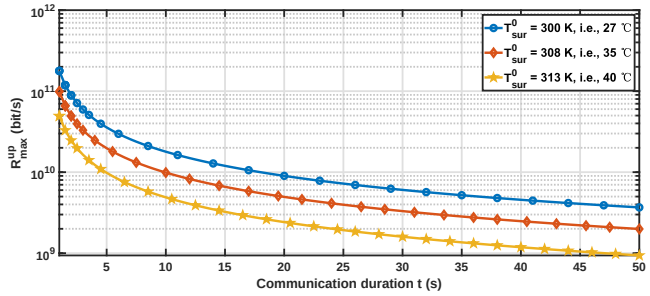

Fig. 7. Upper bound of the maximum receiving rate of smartphones with respect to communication duration.

value of $R_{\max}^{\text{upper}}\left(t\right)$ decreases with the rise of T_{sur}^0.

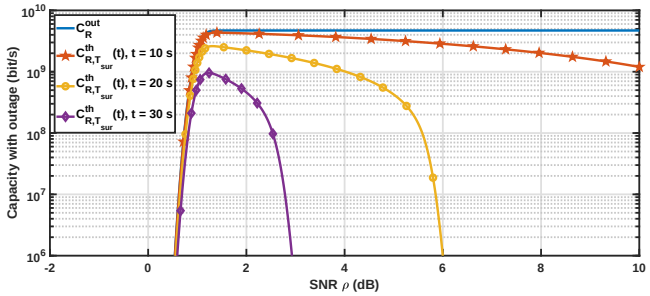

Fig. 8. Capacity with respect to channel outage, i.e., C_R^{out} and $C_{R,T_{\text{sur}}}^{\text{th}}\left(t\right)$, as a function of SNR.

Fig. 8 compares the capacity with respect to channel outage, i.e., C_R^{out} and $C_{R,T_{\text{sur}}}^{\text{th}}\left(t\right)$, in terms of SNR. The results in Fig. 8 indicate that the value of $C_{R,T_{\text{sur}}}^{\text{th}}\left(t\right)$ first grows as SNR increases and then drops after a certain point, which is the maximum value of $C_{R,T_{\text{sur}}}^{\text{th}}\left(t\right)$. The maximum value of $C_{R,T_{\text{sur}}}^{\text{th}}\left(t\right)$ decreases with an extension of the communication duration. Moreover, the results in Fig. 8 indicate that $C_{R,T_{\text{sur}}}^{\text{th}}\left(t\right) \leq C_R^{\text{out}}$.

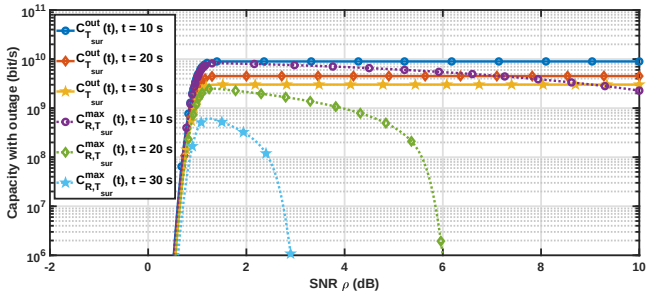

Fig. 9. Capacity performance with power-consumption outage, i.e., $C_{T_{\text{sur}}}^{\text{out}}\left(t\right)$ and $C_{R,T_{\text{sur}}}^{\max}\left(t\right)$, as a function of SNR.

Fig. 9 shows the capacity performance with power-consumption outage, i.e., $C_{T_{\text{sur}}}^{\text{out}}\left(t\right)$ and $C_{R,T_{\text{sur}}}^{\max}\left(t\right)$. These results indicate that the value of $C_{T_{\text{sur}}}^{\text{out}}\left(t\right)$ depends not only on SNR, but also on the communication duration. When the value of SNR is fixed, the value of $C_{T_{\text{sur}}}^{\text{out}}\left(t\right)$ decreases with an extension of the communication duration. Based on the results in Fig. 3, an extension of the communication duration increases the value of $p_{\text{out}}\left[T_{\text{sur}}\left(t\right)\right]$, which causes $C_{T_{\text{sur}}}^{\text{out}}\left(t\right)$ to decrease. When the communication duration is fixed, the value of $C_{T_{\text{sur}}}^{\text{out}}\left(t\right)$ increases as the SNR increases and stays constant when $C_{T_{\text{sur}}}^{\text{out}}\left(t\right)$ reaches maximum value. In the results of Fig. 9, the value of $C_{R,T_{\text{sur}}}^{\max}\left(t\right)$ first grows with the increase of SNR and then

decreases after a certain point which is the maximum value of $C^{\max}_{R,T_{\text{sur}}}(t)$. The maximum value of $C^{\max}_{R,T_{\text{sur}}}(t)$ decreases with an extension of the communication duration. Moreover, the results in Fig. 9 indicate that $C^{\max}_{R,T_{\text{sur}}}(t) \leq C^{\text{out}}_{T_{\text{sur}}}(t)$.

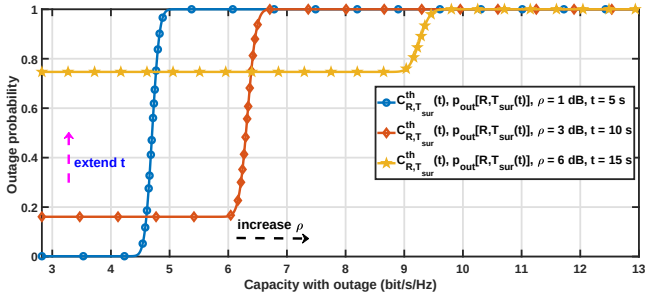

Fig. 10. Normalized capacity with channel outage in joint outage probability, i.e., $C^{\text{th}}_{R,T_{\text{sur}}}(t)/B$, vs. joint outage probability.

Taking into account that -2 dB $\leq \rho_{\text{th}} \leq 10$ dB, Fig. 10 illustrates the normalized capacity with channel outage in the joint outage probability, i.e., $C^{\text{th}}_{R,T_{\text{sur}}}(t)/B$, as a function of joint outage probability $p_{\text{out}}[R, T_{\text{sur}}(t)]$. Fig. 10 shows different curves representing the relationship between the capacity-with-outage versus the outage probability and how they can be influenced by the values of t and ρ. As can be observed, the curves are right-shifted by increasing the SNR or shift up as a result of extending the communication duration.

Based on the simulation results and the model in (13), power-consumption for high data rates mobile applications (e.g., ultra-high-definition live video, virtual reality, and holographic communication) can easily cause outage as a result of excessive local-computations and long execution times.

VI. Conclusions

Power-consumption outage is a phenomenon that causes the working frequency of chips to drop. This is triggered by overheating, which leads to computational overload in mobile devices. Moreover, we specify three features of the power-consumption outage, which are: overheating, decreased frequency, and overload. Furthermore, a power-consumption outage probability is proposed for the first time to evaluate the performance of B5G mobile communication systems. Simulation results indicate that power-consumption outage probability increases with an increase of SNR and an extension of the communication duration. In other words, the joint outage probability of channel and power-consumption outages depends not only on SNR, but also on communication duration. The size of the outage valley in the distribution of joint outage probability shrinks with the rising temperature of the smartphone-back-plate. Moreover, the upper bound of the maximum receiving rate of smartphones decreases with an extension of communication duration. Based on the joint outage probability, the influence of communication duration needs to be considered in the optimization of capacity with outage.

Based on the theoretical results, a design guideline for B5G communication systems is to prevent the occurrence of power-consumption outage at mobile devices. The rationale behind this design guideline is to carefully trade off, among the temperature of chip in mobile devices, downlink rate and communication duration, to reduce the power-consumption outage probability. In future work, we plan to carry out further study to optimize the power-consumption outage probability and compare our results with actual measurements.

Appendix A: Proof of Lemma 1

Proof: Considering the one-dimensional non-steady-state conduction process, the differential equation of heat transfer is given by

$$Q_{\text{Total}} \cdot dt - q \cdot dt = c_{\text{chip}} m \cdot dT_{\text{chip}}, \tag{40}$$

where T_{chip} is the temperature of chip in smartphones, q is the heat dissipation power of chip. Considering the heat conduction of composite materials [28], the heat dissipation of chip is calculated by

$$q = z\left(T_{\text{chip}} - T_{\text{env}}\right), \tag{41}$$

where $z = 1/\left(\frac{L}{k_1 A} + \frac{D}{k_2 A} + \frac{1}{h_{\text{air}} A}\right)$.

Based on (40) and (41), we can get

$$-\frac{dt}{c_{\text{chip}} m} = \frac{dT_{\text{chip}}}{z\left(T_{\text{chip}} - T_{\text{env}}\right) - Q_{\text{Total}}}. \tag{42}$$

The solution of the differential equation (42) is derived as

$$T_{\text{chip}} = \frac{1}{z} Q_{\text{Total}} + T_{\text{env}} + \frac{1}{z} e^{Nz} e^{-\frac{zt}{c_{\text{chip}} m}}, \tag{43}$$

where N is the constant coefficient. Considering the initial state, i.e., $T_{\text{chip}} = T^0_{\text{chip}}$ at $t = 0$, the constant coefficient is derived as

$$N = \frac{1}{z} \ln\left(z T^0_{\text{chip}} - z T_{\text{env}} - Q_{\text{Total}}\right). \tag{44}$$

Based on (43) and (44), the temperature of T_{chip}, varying with the communication duration t, is given by

$$\begin{aligned} T_{\text{chip}} &= \frac{1}{z} Q_{\text{Total}} + T_{\text{env}} + \left(T^0_{\text{chip}} - T_{\text{env}} - \frac{1}{z} Q_{\text{Total}}\right) e^{-\frac{zt}{c_{\text{chip}} m}} \\ &= \frac{1}{z} Q_{\text{Total}} \left(1 - e^{-\frac{zt}{c_{\text{chip}} m}}\right) + T_{\text{env}} + \left(T^0_{\text{chip}} - T_{\text{env}}\right) e^{-\frac{zt}{c_{\text{chip}} m}} \end{aligned}. \tag{45}$$

Based on (14), the relationship between T^0_{chip} and T^0_{sur}, in the case of $t = 0$, is

$$z\left(T^0_{\text{chip}} - T_{\text{env}}\right) = h_{\text{air}} A \left(T^0_{\text{sur}} - T_{\text{env}}\right). \tag{46}$$

Based on (14), (45) and (46), we can get

$$\begin{aligned} T_{\text{sur}} &= \frac{z}{h_{\text{air}} A}\left(T_{\text{chip}} - T_{\text{env}}\right) + T_{\text{env}} \\ &= \frac{z}{h_{\text{air}} A}\left[\frac{1}{z} Q_{\text{Total}} \left(1 - e^{-\frac{zt}{c_{\text{chip}} m}}\right) + \left(T^0_{\text{chip}} - T_{\text{env}}\right) e^{-\frac{zt}{c_{\text{chip}} m}}\right] \\ &\quad + T_{\text{env}} \\ &= \frac{Q_{\text{Total}}}{h_{\text{air}} A}\left(1 - e^{-\frac{zt}{c_{\text{chip}} m}}\right) + \frac{z}{h_{\text{air}} A}\left(T^0_{\text{chip}} - T_{\text{env}}\right) e^{-\frac{zt}{c_{\text{chip}} m}} \\ &\quad + T_{\text{env}} \\ &= \frac{Q_{\text{Total}}}{h_{\text{air}} A}\left(1 - e^{-\frac{zt}{c_{\text{chip}} m}}\right) + \left(T^0_{\text{sur}} - T_{\text{env}}\right) e^{-\frac{zt}{c_{\text{chip}} m}} + T_{\text{env}} \end{aligned}. \tag{47}$$

which completes the proof.

APPENDIX B: PROOF OF THEOREM 1

Proof: Consider that $c(t) \geq 0$, $R_{\max}(t) = \frac{c(t)}{aF_{\text{bit}}+b}$ is the monotonic function for all F_{bit} in the range $\left[0, \frac{c(t)}{b}\right]$. Moreover, $F_{\text{bit}} = h[R_{\max}(t)]$, where $h[R_{\max}(t)] = \frac{c(t)}{aR_{\max}(t)} - \frac{b}{a}$. If the random variable $F_{\text{bit}} \geq 0$ has a gamma distribution with shape parameter α and scale parameter β, the PDF of $R_{\max}(t)$ is derived as

$$\begin{aligned} f[R_{\max}(t)] &= f_{\text{bit}}\{h[R_{\max}(t)]\}\left|\frac{dh[R_{\max}(t)]}{dR_{\max}(t)}\right| \\ &= f_{\text{bit}}\left[\frac{c(t)}{aR_{\max}(t)} - \frac{b}{a}\right]\frac{c(t)}{aR_{\max}^2(t)} \\ &= \frac{c(t)}{a\beta^{\alpha}\Gamma(\alpha)R_{\max}^2(t)}\left(\frac{c(t)}{aR_{\max}(t)} - \frac{b}{a}\right)^{\alpha-1} e^{-\left(\frac{c(t)}{a\beta R_{\max}(t)} - \frac{b}{a\beta}\right)} \end{aligned} \tag{48}$$

Considering that $a > 0$, $b > 0$ and $r \geq 0$, $R_{\max}(t) \leq r$ is equal to $F_{\text{bit}} \geq \frac{c(t)-br}{ar}$. The CDF of $R_{\max}(t)$ is calculated by

$$\begin{aligned} \mathbb{P}[R_{\max}(t) \leq r] &= \mathbb{P}\left[F_{\text{bit}} \geq \frac{c(t)-br}{ar}\right] \\ &= \int_{\Psi} f(F_{\text{bit}})\, dF_{\text{bit}} \end{aligned} \tag{49}$$

where $\Psi = \left\{F_{\text{bit}} | F_{\text{bit}} \geq 0, F_{\text{bit}} \geq \frac{c(t)-br}{ar}\right\}$ is the interval of integration. Defining $\Lambda = \frac{c(t)-br}{ar}$, the value of Λ is analyzed as follows.

When $\Lambda \geq 0$, i.e., $0 \leq r \leq \frac{c(t)}{b}$, the interval of integration is $\Psi = \left\{F_{\text{bit}} | F_{\text{bit}} \geq \frac{c(t)-br}{ar}\right\}$. $\mathbb{P}[R_{\max}(t) \leq r]$ is calculated by

$$\mathbb{P}[R_{\max}(t) \leq r] = \int_{\Lambda}^{\infty} \frac{1}{\beta\Gamma(\alpha)}\left(\frac{F_{\text{bit}}}{\beta}\right)^{\alpha-1} e^{-\frac{F_{\text{bit}}}{\beta}} dF_{\text{bit}}, \tag{50}$$

which indicates that $\mathbb{P}[R_{\max}(t) \leq r]$ is equal to the complementary cumulative distribution function (CCDF) of the random variable F_{bit}.

When $\Lambda < 0$, i.e., $r > \frac{c(t)}{b}$, the interval of integration is $\Psi = \{F_{\text{bit}} | F_{\text{bit}} \geq 0\}$. $\mathbb{P}[R_{\max}(t) \leq r]$ is calculated by

$$\mathbb{P}[R_{\max}(t) \leq r] = \int_{0}^{\infty} \frac{1}{\beta\Gamma(\alpha)}\left(\frac{F_{\text{bit}}}{\beta}\right)^{\alpha-1} e^{-\frac{F_{\text{bit}}}{\beta}} dF_{\text{bit}} = 1. \tag{51}$$

which completes the proof.

APPENDIX C: PROOF OF LEMMA 2

Proof: Considering that the event $T_{\text{sur}}(t) < T_{\text{safe}}$ is equal to the event $R < R_{\max}(t)$, we get that $\mathbb{P}[R < R_{\text{th}}, T_{\text{sur}}(t) < T_{\text{safe}}] = \mathbb{P}[R < R_{\text{th}}, R < R_{\max}(t)]$.

Based on **Theorem 2**, $\mathbb{P}[R < R_{\text{th}}, R < R_{\max}(t)]$ is derived as

$$\begin{aligned} &\mathbb{P}[R < R_{\text{th}}, R < R_{\max}(t)] \\ &= \mathbb{E}\{\mathbb{P}[R < R_{\text{th}}, R < R_{\max}(t) | R_{\max}(t)]\} = \\ &\int_0^{\frac{c(t)}{b}} \mathbb{P}[R < R_{\text{th}}, R < R_{\max}(t) | R_{\max}(t)] f[R_{\max}(t)] dR_{\max}(t) \end{aligned} \tag{52}$$

On the condition of $0 < R_{\text{th}} \leq \frac{c(t)}{b}$, $\mathbb{P}[R < R_{\text{th}}, R < R_{\max}(t)]$ is calculated by

$$\begin{aligned} &\mathbb{P}[R < R_{\text{th}}, R < R_{\max}(t)] \\ &= \int_0^{R_{\text{th}}} \mathbb{P}[R < R_{\max}(t) | R_{\max}(t)] f[R_{\max}(t)] dR_{\max}(t) \\ &\quad + \int_{R_{\text{th}}}^{\frac{c(t)}{b}} \mathbb{P}[R < R_{\text{th}} | R_{\max}(t)] f[R_{\max}(t)] dR_{\max}(t) \end{aligned} \tag{53}$$

where

$$\mathbb{P}[R < R_{\max}(t) | R_{\max}(t)] = \frac{1}{2} + \frac{1}{2}\text{erf}\left(\frac{R_{\max}(t) - B\mu}{B\theta\sqrt{2}}\right) \tag{54}$$

and

$$\begin{aligned} \mathbb{P}[R < R_{\text{th}} | R_{\max}(t)] &= \frac{1}{2} + \frac{1}{2}\text{erf}\left(\frac{R_{\text{th}} - B\mu}{B\theta\sqrt{2}}\right). \\ &= \mathbb{P}[R < R_{\text{th}}] = p_{\text{out}}(R) \end{aligned} \tag{55}$$

Considering that $\mathbb{P}[R_{\max}(t) > R_{\text{th}}] = \int_{R_{\text{th}}}^{\frac{c(t)}{b}} f[R_{\max}(t)] dR_{\max}(t)$, the equation (52) is converted to

$$\begin{aligned} &\mathbb{P}[R < R_{\text{th}}, R < R_{\max}(t)] \\ &= \int_0^{R_{\text{th}}} \left[\frac{1}{2} + \frac{1}{2}\text{erf}\left(\frac{R_{\max}(t) - B\mu}{B\theta\sqrt{2}}\right)\right] f[R_{\max}(t)] dR_{\max}(t). \\ &\quad + p_{\text{out}}(R)\, \mathbb{P}[R_{\max}(t) > R_{\text{th}}] \end{aligned} \tag{56}$$

On the condition of $R_{\text{th}} > \frac{c(t)}{b}$, $\mathbb{P}[R < R_{\text{th}}, R < R_{\max}(t)]$ is calculated by

$$\begin{aligned} &\mathbb{P}[R < R_{\text{th}}, R < R_{\max}(t)] \\ &= \int_0^{\frac{c(t)}{b}} \mathbb{P}[R < R_{\max}(t) | R_{\max}(t)] f[R_{\max}(t)] dR_{\max}(t) \\ &= \int_0^{\frac{c(t)}{b}} \left[\frac{1}{2} + \frac{1}{2}\text{erf}\left(\frac{R_{\max}(t) - B\mu}{B\theta\sqrt{2}}\right)\right] f[R_{\max}(t)] dR_{\max}(t), \\ &\overset{(a)}{=} \frac{1}{2} + \frac{\int_0^{\infty} \text{erf}\left[\frac{X(F_{\text{bit}},t)-\mu}{\theta\sqrt{2}}\right](F_{\text{bit}})^{\alpha-1} e^{-\frac{F_{\text{bit}}}{\beta}} dF_{\text{bit}}}{2(\beta)^{\alpha}\Gamma(\alpha)} \end{aligned} \tag{57}$$

where $X(F_{\text{bit}}, t) = \frac{R_{\max}(t)}{B}$, (a) is calculated based on **Theorem 2** and $R_{\max}(t) = \frac{c(t)}{aF_{\text{bit}}+b}$. Based on **Theorem 1**, we can obtain

$$\begin{aligned} \mathbb{P}[R < R_{\text{th}}, R < R_{\max}(t)] &= 1 - \mathbb{P}[T_{\text{sur}}(t) \geq T_{\text{safe}}] \\ &= \mathbb{P}[T_{\text{sur}}(t) < T_{\text{safe}}] \end{aligned} \tag{58}$$

which completes the proof.

REFERENCES

[1] V. Petrov *et al.*, "Last Meter Indoor Terahertz Wireless Access: Performance Insights and Implementation Roadmap," *IEEE Communications Magazine*, vol. 56, no. 6, pp. 158-165, 2018.

[2] M. Xiao *et al.*, "Millimeter Wave Communications for Future Mobile Networks," *IEEE Journal on Selected Areas in Communications*, vol. 35, no. 9, pp. 1909-1935, 2017.

[3] X. Ge *et al.*, "Joint Optimization of Computation and Communication Power in Multi-user Massive MIMO Systems," *IEEE Transactions on Wireless Communications*, pp. 1-1, 2018.

[4] X. Ge *et al.*, "5G Ultra-Dense Cellular Networks," *IEEE Wireless Communications*, vol. 23, no. 1, pp. 72-79, 2016.

[5] J. Yang *et al.*, "How Much of Wireless Rates Can Smartphones Support in 5G Networks?," *IEEE Network*, vol. 33, no. 3, pp. 122-129, 2019.

[6] J. Yang *et al.*, "Power-Consumption Outage Challenge in Next-Generation Cellular Networks," in *2019 IEEE Global Communications Conference (GLOBECOM)*, 2019, pp. 1-6.
[7] A. Goldsmith, *Wireless communications*. Cambridge university press, 2005.
[8] S. V. Garimella *et al.*, "Electronics Thermal Management in Information and Communications Technologies: Challenges and Future Directions," *IEEE Transactions on Components, Packaging and Manufacturing Technology*, vol. 7, no. 8, pp. 1191-1205, 2017.
[9] E. Ungar and K. Stroud, "A New Approach to Defining Human Touch Temperature Standards," in *40th International Conference on Environmental Systems*(International Conference on Environmental Systems (ICES): American Institute of Aeronautics and Astronautics, 2010.
[10] Q. Ding and Y. Jing, "Outage Probability Analysis and Resolution Profile Design for Massive MIMO Uplink With Mixed-ADC," *IEEE Transactions on Wireless Communications*, vol. 17, no. 9, pp. 6293-6306, 2018.
[11] B. M. ElHalawany *et al.*, "D2D Communication for Enabling Internet-of-Things: Outage Probability Analysis," *IEEE Transactions on Vehicular Technology*, vol. 68, no. 3, pp. 2332-2345, 2019.
[12] K. J. Kim *et al.*, "Outage Probability Analysis of Spectrum Sharing Systems With Distributed Cyclic Delay Diversity," *IEEE Transactions on Communications*, vol. 67, no. 6, pp. 4435-4449, 2019.
[13] J. Cui *et al.*, "Outage Probability Constrained MIMO-NOMA Designs Under Imperfect CSI," *IEEE Transactions on Wireless Communications*, vol. 17, no. 12, pp. 8239-8255, 2018.
[14] N. Cheng *et al.*, "Performance Analysis of Vehicular Device-to-Device Underlay Communication," *IEEE Transactions on Vehicular Technology*, vol. 66, no. 6, pp. 5409-5421, 2017.
[15] M. C. Valenti *et al.*, "The role of computational outage in dense cloud-based centralized radio access networks," in *2014 IEEE Global Communications Conference*, 2014, pp. 1466-1472.
[16] D. Han *et al.*, "Offloading Optimization and Bottleneck Analysis for Mobile Cloud Computing," *IEEE Transactions on Communications*, vol. 67, no. 9, pp. 6153-6167, 2019.
[17] M. Liu *et al.*, "Cooperative Fog-Cloud Computing Enhanced by Full-Duplex Communications," *IEEE Communications Letters*, vol. 22, no. 10, pp. 2044-2047, 2018.
[18] X. Li *et al.*, "Measurement and analysis of energy consumption on Android smartphones," in *2014 4th IEEE International Conference on Information Science and Technology*, 2014, pp. 242-245.
[19] P. K. D. Pramanik *et al.*, "Power Consumption Analysis, Measurement, Management, and Issues: A State-of-the-Art Review of Smartphone Battery and Energy Usage," *IEEE Access*, vol. 7, pp. 182113-182172, 2019.
[20] R. W. Ahmad *et al.*, "A survey on energy estimation and power modeling schemes for smartphone applications," *International Journal of Communication Systems*, vol. 30, no. 11, p. e3234, 2017.
[21] P. M. Hell *et al.*, "Mobile Phones Thermo-Ergonomic Analysis," in *2018 IEEE 16th International Symposium on Intelligent Systems and Informatics (SISY)*, 2018, pp. 000249-000254.
[22] M. Ishii and Y. Nakashima, "Development of algorithms for real-time estimation of smartphone surface temperature using embedded processor," in *2017 16th IEEE Intersociety Conference on Thermal and Thermomechanical Phenomena in Electronic Systems (ITherm)*, 2017, pp. 1088-1093.
[23] Q. Xie *et al.*, "Therminator: A thermal simulator for smartphones producing accurate chip and skin temperature maps," in *2014 IEEE/ACM International Symposium on Low Power Electronics and Design (ISLPED)*, 2014, pp. 117-122.
[24] G. P. Srinivasa, "A Temperature-Aware Approach to Managing Smartphone Efficiency and Power Consumption," Ph.D., State University of New York at Buffalo, Ann Arbor, 22616749, 2019.
[25] E. A. Jorswieck and H. Boche, "Outage probability in multiple antenna systems," *European Transactions on Telecommunications*, vol. 18, no. 3, pp. 217-233, 2007.
[26] B. M. Hochwald *et al.*, "Multiple-antenna channel hardening and its implications for rate feedback and scheduling," *IEEE Transactions on Information Theory*, vol. 50, no. 9, pp. 1893-1909, 2004.
[27] Y. Long *et al.*, "Minimum Number of Antennas Required to Satisfy Outage Probability in Massive MIMO Systems," *IEEE Wireless Communications Letters*, vol. 5, no. 4, pp. 348-351, 2016.
[28] T. L. Bergman *et al.*, *Fundamentals of heat and mass transfer*. John Wiley & Sons, 2011.
[29] F. Paterna *et al.*, "Ambient variation-tolerant and inter components aware thermal management for mobile system on chips," presented at the *Proceedings of the conference on Design, Automation & Test in Europe*, Dresden, Germany, 2014.
[30] E. Bjornson *et al.*, "Optimal Design of Energy-Efficient Multi-User MIMO Systems: Is Massive MIMO the Answer?," *IEEE Transactions on Wireless Communications*, vol. 14, no. 6, pp. 3059-3075, 2015.
[31] C. H. Bennett, "Notes on Landauer's principle, reversible computation, and Maxwell's Demon," *Studies in History and Philosophy of Modern Physics*, vol. 34B, no. 3, pp. 501-510, Sep 2003.
[32] Y. A. Cengel and M. A. Boles, *Thermodynamics: an engineering approach*, 5th ed. Boston : McGraw-Hill, 2002.
[33] M. H. Suzer and K. D. Kang, "Predictive Thermal Control for Real-Time Video Decoding," in *2014 26th Euromicro Conference on Real-Time Systems*, 2014, pp. 233-242.
[34] V. Zhirnov *et al.*, "Minimum Energy of Computing, Fundamental Considerations," in *ICT - Energy - Concepts Towards Zero - Power Information and Communication Technology*, 2014.
[35] W. Yuan and K. Nahrstedt, "Energy-efficient CPU scheduling for multimedia applications," *ACM Transactions on Computer Systems*, Article vol. 24, no. 3, pp. 292-331, 2006.
[36] W. Zhang *et al.*, "Energy-Optimal Mobile Cloud Computing under Stochastic Wireless Channel," *IEEE Transactions on Wireless Communications*, vol. 12, no. 9, pp. 4569-4581, 2013.
[37] G. Li *et al.*, "Energy-efficient fuzzy control model for GPU-accelerated packet classification," *Concurrency and Computation: Practice and Experience*, vol. 29, no. 17, p. e4079, 2017.
[38] J. Park and H. Cha, "Aggressive Voltage and Temperature Control for Power Saving in Mobile Application Processors," *IEEE Transactions on Mobile Computing*, vol. 17, no. 6, pp. 1233-1246, 2018.
[39] Q. Xie *et al.*, "Dynamic thermal management in mobile devices considering the thermal coupling between battery and application processor," in *2013 IEEE/ACM International Conference on Computer-Aided Design (ICCAD)*, 2013, pp. 242-247.
[40] C. M. Velpula *et al.*, "CPU temperature aware scheduler a study on incorporating temperature data for CPU scheduling decisions," in *2015 International Conference on Advances in Computing, Communications and Informatics (ICACCI)*, 2015, pp. 2409-2413.
[41] C. Qiu *et al.*, "Scaling carbon nanotube complementary transistors to 5-nm gate lengths," *Science*, vol. 355, no. 6322, pp. 271-276, 2017.
[42] S. D. Ji *et al.*, "Effect of Temperature on Material Transfer Behavior at Different Stages of Friction Stir Welded 7075-T6 Aluminum Alloy," *Journal of Materials Science & Technology*, vol. 29, no. 10, pp. 955-960, 2013.

Jing Yang (S'17) received the B.E. degree in communication engineering from Huazhong University of Science and Technology (HUST),Wuhan, China, in 2014. He is currently pursuing the Ph.D. degree at HUST. His research interests mainly include computation power of wireless communication systems, green communication, energy efficiency of wireless cellular networks, and Landauer principle.

Xiaohu Ge (M'09-SM'11) received the Ph.D. degree in communication and information engineering from the Huazhong University of Science and Technology (HUST), China, in 2003. He has been worked with HUST, since November 2005. Prior to that, he worked as a Researcher at Ajou University, South Korea, and the Politecnico Di Torino, Italy, from January 2004 to October 2005. He is currently a full Professor with the School of Electronic Information and Communications, HUST. He is also an Adjunct Professor with the Faculty of Engineering and Information Technology, University of Technology Sydney (UTS), Australia. He has published about 200 articles in refereed journals and conference proceedings. He has been granted about 25 patents in China. His research interests are in the area of mobile communications, traffic modeling in wireless networks, green communications, and interference modeling in wireless communications. He services as an IEEE Distinguished Lecturer and an Associate Editor for the IEEE Access, the IEEE Wireless Communications and the IEEE Transactions on Vehicular Technology, etc.

John Thompson (F16) is currently a Professor at the School of Engineering in the University of Edinburgh. He specializes in antenna array processing, cooperative communications systems, energy efficient wireless communications and their applications. He has published in excess of three hundred and fifty papers on these topics. In 2018, he was the co-chair of the IEEE Smartgridcomm conference held in Aalborg, Denmark. He currently participates in a UK research project which studies new concepts for signal processing. In January 2016, he was elevated to Fellow of the IEEE for contributions to antenna arrays and multi-hop communications. In 2015-2018, he has been recognised by Thomson Reuters as a highly cited researcher.

Hamid Gharavi received his Ph.D. degree from Loughborough University, United Kingdom, in 1980. He joined the Visual Communication Research Department at AT&T Bell Laboratories, Holmdel, New Jersey, in 1982. He was then transferred to Bell Communications Research (Bellcore) after the AT&T-Bell divestiture, where he became a consultant on video technology and a Distinguished Member of Research Staff. In 1993, he joined Loughborough University as a professor and chair of communication engineering. Since September 1998, he has been with the National Institute of Standards and Technology (NIST). He was a core member of Study Group XV (Specialist Group on Coding for Visual Telephony) of the International Communications Standardization Body CCITT (ITU-T). His research interests include smart grid, wireless multimedia, mobile communications and wireless systems, mobile ad hoc networks, and visual communications. He holds eight U.S. patents and has over 150 publications related to these topics. He received the Charles Babbage Premium Award from the Institute of Electronics and Radio Engineering in 1986, and the IEEE CAS Society Darlington Best Paper Award in 1989. He served as a Distinguished Lecturer of the IEEE Communication Society. He was the recipient of the Washington Academy of Science Distinguished Career in Science Award for 2017.He has been a Guest Editor for a number of special issues of the Proceedings of the IEEE, including Smart Grid, Sensor Networks & Applications, Wireless Multimedia Communications, Advanced Automobile Technologies, and Grid Resilience. He was a TPC Co-Chair for IEEE SmartGridComm in 2010 and 2012, as well as IEEE GLOBECOM 2019. He served as a member of the Editorial Board of Proceedings of the IEEE from January 2003 to December 2008. From January 2010 to December 2013 he served as Editor-in-Chief of IEEE Transactions on CAS for Video Technology and the Editor-in-Chief of IEEE Wireless Communications.